

Disconnected entanglement entropy as a marker of edge modes in a periodically driven Kitaev chain

Saikat Mondal^{1,*}, Diptiman Sen^{2,†} and Amit Dutta^{1‡}

¹*Department of Physics, Indian Institute of Technology, Kanpur 208016, India*

²*Centre for High Energy Physics and Department of Physics,
Indian Institute of Science, Bengaluru 560012, India*

We study the disconnected entanglement entropy (DEE) of a Kitaev chain in which the chemical potential is periodically modulated. In this driving protocol, the DEE of a sufficiently large system with open boundary conditions turns out to be integer-quantized, with the integer being equal to the number of Majorana edge modes generated by the periodic driving. Thus, the DEE can be considered as a marker for detecting Majorana edge modes in a periodically driven Kitaev chain. Using the DEE, we further show that these Majorana edge modes are robust against weak spatial disorder and temporal noise. Interestingly, we find that the DEE may, in some cases, also detect the anomalous edge modes which can be generated by periodic driving of the nearest-neighbor hopping, even though such modes have no topological significance. We illustrate that these anomalous edge modes are not robust against weak spatial disorder and they disappear in the presence of weak spatial disorder, as manifested in the DEE.

I. INTRODUCTION

There is a recent upsurge in studies of topological phases of matter [1–6]. These phases are robust against weak perturbations due to the existence of a bulk gap, which does not vanish unless the system crosses a gapless quantum critical point (QCP). In addition, a topological phase is characterized by a topological invariant, which remains constant under continuous variations of parameters as long as the system remains in the same phase and becomes ill-defined at QCPs which separate different phases.

In this regard, the Kitaev chain of spinless fermions (a p -wave superconducting system in one dimension) is a paradigmatic model that hosts symmetry protected topologically non-trivial and topologically trivial phases separated by a QCP [7, 8]. The topological properties of a Kitaev chain with periodic boundary conditions is characterized by a topological invariant known as the winding number. The winding number assumes non-zero integer-quantized values in the topologically non-trivial phase and vanishes in the topologically trivial phase. For a system with open boundary conditions, the topologically non-trivial phase of the model is manifested in the existence of zero-energy Majorana modes localized at the edges; on the contrary, the topologically trivial phase does not host Majorana edge modes. The exact solvability of the model has been extensively exploited to understand its equilibrium as well as out-of-equilibrium properties [7–17].

Concerning the non-equilibrium dynamics of closed quantum systems, periodically driven systems have been explored both in the context of thermalization [18–28]

and emergent topology [10, 11, 15, 17, 29–50] (for recent review articles, see Refs. [17, 21, 26, 28]). For a periodically driven Kitaev chain with open boundary conditions, it has been shown that Majorana edge modes (zero and π -modes) can be dynamically generated [11, 15, 17] even though the instantaneous Hamiltonian may remain topologically trivial at all times. In fact, it is the effective Floquet Hamiltonian [51] that determines the non-trivial topology (i.e., the existence of zero-energy Majorana edge modes) of a driven chain. It has been observed that the number of such dynamical edge modes increases as the drive frequency is reduced. Further, a strong (having a sufficiently large amplitude) periodic modulation of the hopping parameter can produce some “anomalous” edge modes with non-zero Floquet quasienergies [15]. However, the anomalous edge modes are not Floquet Majorana modes. These modes have no topological significance and topological invariants like the winding number miss them completely. Furthermore, as we elaborate in this work, these modes are not robust against weak spatial disorder.

There have been several attempts to characterize the out-of-equilibrium topology of one-dimensional systems (e.g., the Kitaev chain and the Su-Schrieffer-Heeger chain) using the dynamical winding number calculated from the instantaneous wave function of the system [52–54]. In a periodically driven Kitaev chain, the corresponding winding number [11] is calculated from the Floquet Hamiltonian (for a review, see Ref. [17]). This winding number correctly predicts the number of zero-energy Majorana modes for a Kitaev chain with a periodically driven chemical potential. However, the dynamical winding number fails to detect the anomalous edge modes which arise when the hopping parameter is driven strongly [15].

Recently, the notion of a disconnected entanglement entropy (DEE) [55, 56] has been introduced which plays a role similar to a topological invariant in an equilibrium Kitaev chain with an open boundary condition. It is

* msaikat@iitk.ac.in

† diptiman@iisc.ac.in

‡ dutta@iitk.ac.in

worth noting that unlike the winding number, the DEE is not a bulk topological invariant. Rather, it extracts the entanglement between the Majorana modes localized at the edges. Although the DEE can take any real value by its construction, it turns out to be integer-quantized for a short-ranged Kitaev chain in the topological phase, where the integer is the total number of edge modes of the system [55–57].

In this paper, we explore the efficacy of the DEE in detecting the dynamically generated edge modes for a periodically driven Kitaev chain. We study the variation of the DEE with the drive frequency for three different types of periodic modulations of the chemical potential, namely, δ -pulses, (and also square pulse and sinusoidal variations). Our study establishes that the DEE correctly predicts the number of edge modes. We also investigate the applicability of the DEE as a marker of anomalous edge modes appearing due to a periodic modulation of the nearest-neighbor hopping amplitude.

It is also noteworthy that the verification of topological properties of periodically driven systems are experimentally more viable compared to undriven systems. Recently, the periodic driving protocol of a (kicked) transverse field Ising model has been implemented experimentally using an array of superconducting qubits [58]. It is important to note that this model can be mapped to a Kitaev chain through Jordan-Wigner transformations [59] and thus this model can host Majorana edge modes. In the present work, we not only probe how these Floquet Majorana modes are manifested in the DEE, but also we illustrate the robustness of these modes against weak spatial disorder and temporal noise.

The rest of the paper is organized as follows: the conventional definition of the DEE is introduced in Sec. II. In Sec. III, we briefly recapitulate a short-ranged Kitaev chain of spinless fermions and its topological properties. The behavior of the DEE for a Kitaev chain with periodically modulated chemical potential is explored in Sec. IV. We analyze the effects of spatial disorder and temporal noise in the periodic driving on the DEE in Sec. V. In Sec. VI, we study the situation where the nearest-neighbor hopping amplitude is periodically modulated and address the question of whether the DEE can detect the anomalous edge modes. Concluding remarks are presented in Section VII. The definition of the winding number of a short-range (static) Kitaev chain is given in Appendix A. The methods used for computing the DEE from Floquet Hamiltonian are explained in Appendix B. We present the behavior of the DEE for periodic driving with a square pulse and a sinusoidal modulation in Appendix C. We then briefly compare the DEE with the dynamical winding number derived from the Floquet Hamiltonian for a periodic variation of the chemical potential in Appendix D. In Appendix E, we provide an analytical derivation of the frequencies at which Floquet quasienergy gap closes, choosing the example of the periodic driving of the hopping amplitude.

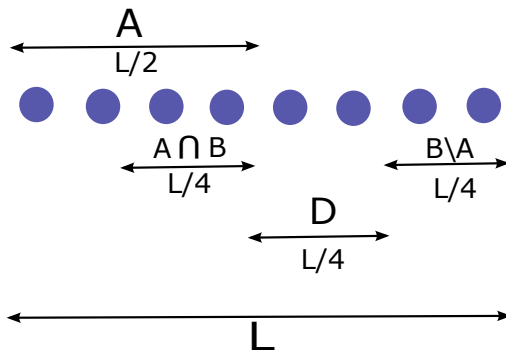


FIG. 1. Partitions of a chain with the disconnected partition $D = \overline{A \cup B}$ and $2L_A = 2L_B = 4L_D = L$. The subsystem B consists of two partitions $A \cap B$ and $B \setminus A$, separated by the disconnected partition D (Ref. [57]).

II. DISCONNECTED ENTANGLEMENT ENTROPY

In this section, we briefly introduce the notion of disconnected entanglement entropy (DEE) [55, 56]. To this end, we first consider a composite system \mathcal{S} that is in a pure state and is described by a density matrix ρ . The reduced density matrix of a subsystem A is obtained by tracing over the degrees of freedom of the rest of the system \overline{A} [60]:

$$\rho_A = \text{Tr}_{\overline{A}}(\rho). \quad (1)$$

The entanglement entropy [61–64] of subsystem A is then defined in terms of the eigenvalues α_i of the reduced density matrix ρ_A as

$$S_A = -\text{Tr}_A(\rho_A \ln(\rho_A)) = -\sum_i \alpha_i \ln(\alpha_i). \quad (2)$$

As the system \mathcal{S} is in a pure state, it can be shown that $S_A = S_{\overline{A}}$.

We now consider a configuration of the partitions A , B , $A \cap B$ and $A \cup B$ of the system \mathcal{S} , such that the subsystem B consists of two parts $A \cap B$ and $B \setminus A$, separated by the disconnected partition $D = \overline{A \cup B}$, as shown in Fig. 1. The DEE [55–57] is then defined as

$$S_D = S_A + S_B - S_{A \cup B} - S_{A \cap B}. \quad (3)$$

III. SHORT-RANGE KITAEV CHAIN

We recall the Hamiltonian of a Kitaev chain [7–11] with short-ranged interactions given by

$$H = -\gamma \sum_{n=1}^{L-1} (c_n^\dagger c_{n+1} + c_{n+1}^\dagger c_n) - \mu \sum_{n=1}^L (2c_n^\dagger c_n - 1) + \Delta \sum_{n=1}^{L-1} (c_n c_{n+1} + c_{n+1}^\dagger c_n^\dagger), \quad (4)$$

where c_n (c_n^\dagger) is the annihilation (creation) operator for a spinless fermion on the n -th site, γ is the nearest-neighbor hopping parameter, Δ is the strength of the p -wave superconducting pairing, and μ is the on-site chemical potential. The parameters γ , Δ and μ will be taken to be real unless otherwise mentioned. Consequently, the Hamiltonian respects time-reversal symmetry (\mathcal{T}), particle-hole symmetry (\mathcal{P}) and sub-lattice/chiral symmetry (\mathcal{C}) and the system belongs to the BDI symmetry class. Definition of the winding number and topological properties of a short-range Kitaev chain are briefly discussed in Appendix A.

It is noteworthy that in a chain with short-ranged couplings and open boundary conditions, the DEE, calculated in the ground state of static Hamiltonian, is an integer multiple of $\ln(2)$, i.e., $S_D = p \ln(2)$, where p is the total number of modes at the edges of an open chain (see Ref. [55–57]). The total number of edge modes is twice the number of modes at each edge. Therefore, the values of the DEE in the topologically non-trivial ($-1 < \mu < 1$) and trivial ($|\mu| > 1$) phases of a Kitaev chain are $2 \ln(2)$ and zero, respectively, and there is a discontinuous jump in the value of the DEE at the QCP separating the two phases. Thus, the DEE plays a role equivalent to the winding number for an open chain.

IV. DEE FOR A KITAEV CHAIN WITH PERIODICALLY MODULATED CHEMICAL POTENTIAL

In this section, we discuss the behavior of the DEE calculated in the ground state of the effective Floquet Hamiltonian for a Kitaev chain with a periodically modulated chemical potential.

We consider a Kitaev chain with an open boundary condition in which the chemical potential is periodically modulated [11], such that $\mu(t) = \mu(t + T)$, with $T = 2\pi/\omega$, where ω is the driving frequency, so that $H(t)$ in Eq. (4) satisfies $H(t) = H(t + T)$. For a time-periodic Hamiltonian $H(t)$, the stroboscopic time-evolution operator (i.e., the Floquet operator) is defined as

$$U_F = \mathbb{T} \exp \left(-i \int_0^T H(t) dt \right) = \exp(-iH_F T), \quad (5)$$

where H_F is the Floquet Hamiltonian and \mathbb{T} denotes time-ordering. (We will set $\hbar = 1$ in this paper).

We recall that due to the unitary nature of the Floquet operator U_F , its eigenvalues are phases. Further, these appear in complex conjugate pairs, $e^{i\theta}$ and $e^{-i\theta}$ (see Appendix B for details). If present, Majorana edge modes correspond to the eigenvalues $+1$ and -1 of the Floquet operator (U_F). In other words, their corresponding Floquet quasienergies are $\epsilon_F = 0$ and $\epsilon_F = \pm\pi/T$, respectively. Thus, the number of Majorana edge modes is given by the total number of eigenvalues $+1$ and -1 of U_F .

We now consider the protocol in which the chemical potential μ is periodically modulated by the application of δ -pulses such that [11, 17]

$$\mu(t) = \mu_0 + \mu_1 \sum_{m=-\infty}^{\infty} \delta(t - mT), \quad (6)$$

where $T = 2\pi/\omega$. For this driving protocol, the DEE is calculated in the ground state of the Floquet Hamiltonian H_F , where all the single-particle negative quasienergy states are filled and all the single-particle positive quasienergy states are empty. The methods used to calculate the DEE from the correlation matrix are explained in Appendix B. In this driving protocol, the DEE, calculated in the ground state of the Floquet Hamiltonian, is equal to integer multiples of $\ln(2)$, as can be seen from Fig. 2(a). Thus, $S_D = p \ln(2)$, where p is the total number of Majorana edge modes (both zero and π -modes). It is also interesting to note that the DEE generally increases as the drive frequency ω decreases. Further, we have verified that the value of $S_D/\ln(2)$ is equal to the number of Majorana modes (see Fig. 2(b)) generated by the same periodic driving of the Kitaev chain. We reiterate that the number of Majorana modes is counted from the total number of eigenvalues $+1$ and -1 of the Floquet operator U_F .

However, at low drive frequencies (i.e., when ω is of the order of the hopping parameter γ), the DEE is not integer-quantized and the value of $S_D/\ln(2)$ differs significantly from the number of Majorana end modes. This is however a finite-size effect, as shown in Fig. 3, which demonstrates that the DEE does saturate to an integer-quantized value for large system size L . The reason for the finite-size effect is that at low frequencies, the decay lengths of the Majorana edge modes increase and therefore the edge modes mix more and more with the bulk states. When the decay length is comparable to the size $L/4$ of the disconnected region D , the contribution of such end modes to the DEE deviates from integer multiples of $\ln(2)$. This leads to the reduction of the entanglement between the edge modes. On the other hand, at low frequencies, the bulk states become long-range entangled (as the effective range of couplings appearing in the Floquet Hamiltonian increases with decreasing drive frequency) and contribute to the DEE computed from the Floquet Hamiltonian. For small ω , therefore, the deviation of the DEE from integer-quantized value occurs due to the competition between these two contradictory effects. As the length $L_D = L/4$ is increased, the bulk contribution to the DEE decreases. Also, with the increase of L , the dispersion of the edge modes to the bulk states decreases, even at low drive frequencies. Thus, for sufficiently large L (and therefore sufficiently large $L_D = L/4$), the bulk contribution becomes negligibly small and the DEE only contains the integer-quantized contribution of the edge modes.

We also observe a similar behavior of the DEE for periodic modulation of the chemical potential with a square

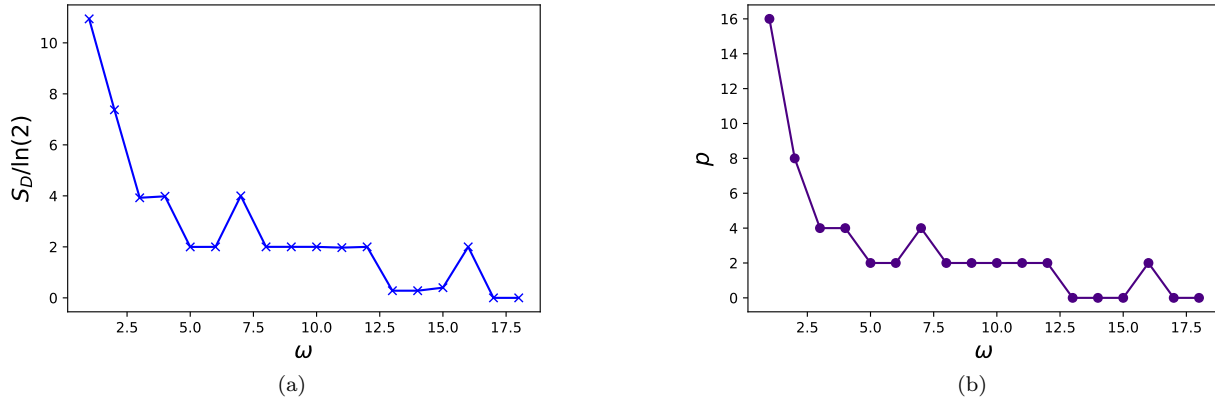


FIG. 2. (a) DEE (S_D) in units of $\ln(2)$ and (b) total number of Majorana edge modes p as functions of driving frequency ω (in the units of the hopping parameter γ , which is set equal to unity) for a Kitaev chain in which the chemical potential μ is periodically modulated by δ -pulses (Eq. (6)) having $\mu_0 = 2.5$ and $\mu_1 = 0.2$. We have taken $L = 200$ and $L_D = 50$. The DEE assumes integer-quantized values except at low frequencies. The number of dynamically generated edge Majorana modes increases as ω decreases.

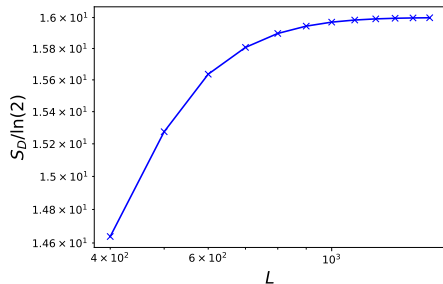


FIG. 3. DEE (S_D) in units of $\ln(2)$ as a function of the length L (in log-log scale) of a Kitaev chain (with $L_D = L/4$) in which the chemical potential μ is periodically modulated by δ -pulses (Eq. (6)) having $\mu_0 = 2.5$, $\mu_1 = 0.2$, and $\omega = 1$. We observe a saturation to an integer-quantized value as L increases establishing that the discrepancy observed for low ω in Fig. 2 is a finite-size effect.

pulse and sinusoidal variation, as shown in Appendix C. Further, the DEE is equivalent to the dynamical (Floquet) winding number in counting the number of emergent Floquet Majorana modes; this is discussed in Appendix D.

V. DEE FOR PERIODIC MODULATION OF CHEMICAL POTENTIAL IN PRESENCE OF SPATIAL DISORDER AND TEMPORAL NOISE

In this section, we discuss the behavior of the DEE for a periodically driven Kitaev chain in the presence of spatial disorder as well as temporal noise, and we establish that the Floquet Majorana modes are robust against weak spatial and temporal disorder.

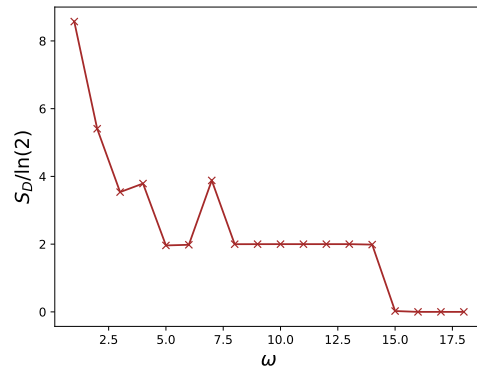


FIG. 4. DEE (S_D) in units of $\ln(2)$ as a function of ω for the driving protocol in the presence of spatial disorder, as in Eq. (7). Here, we have chosen $\mu_0 = 2.5$, $r = 0.2$, $L = 200$ and $L_D = 50$. β_n assumes a random value in the range $[0, 1]$. Here, S_D has been calculated after taking average over a large number of configurations of random numbers.

A. DEE for periodic driving in presence of spatial disorder

We consider a driving protocol where the on-site potentials $\mu_n(t)$ for different sites are driven with δ -pulses of random amplitudes, such that the translational symmetry of the chain is explicitly broken. Therefore, we consider the following form of the chemical potential,

$$\mu_n(t) = \mu_0 + r\beta_n \sum_{m=-\infty}^{\infty} \delta(t - mT), \quad (7)$$

where n denotes the site number in the chain, μ_0 and r are independent of n , and β_n can assume a random value

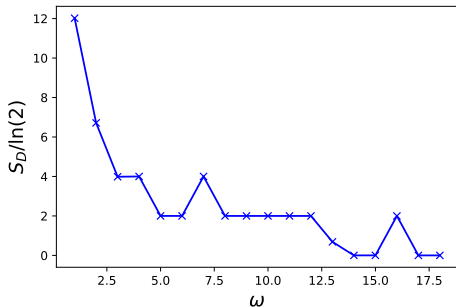


FIG. 5. DEE (S_D) in units of $\ln(2)$ as a function of ω for the driving protocol in the presence of temporal noise, as in Eq. (8). Here, we have chosen $\mu_0 = 2.5$, $\mu_1 = 0.2$, $r = 0.2$, $L = 200$ and $L_D = 50$. $f(t)$ assumes a random value in the range $[-1, 1]$ at any time t .

in the range $[0, 1]$.

After taking the average over a large number of configurations of random numbers, we find that the value of the DEE, calculated in the ground state of the effective Floquet Hamiltonian, remains perfectly integer-quantized even in the presence of weak spatial disorder for high frequency (see Fig. 4). This demonstrates the robustness of Floquet Majorana modes (both zero and π -modes) against weak disorder. However, the deviation of the DEE from integer-quantized value at sufficiently low-frequency is due to the finiteness of the system, as we have elaborated in Fig. 3 for the driving protocol without spatial disorder.

B. DEE for periodic driving in presence of temporal noise

We now consider a driving protocol where the chemical potential $\mu(t)$ is spatially uniform, but is driven with δ -pulses in the presence of a random noise $f(t)$ of sufficiently small amplitude r . We consider the following form of the chemical potential,

$$\mu(t) = \mu_0 + \mu_1 \sum_{n=-\infty}^{\infty} \delta(t - nT) + r f(t), \quad (8)$$

where the function $f(t)$ assumes a random value between $[-1, 1]$ at any time t .

For this driving protocol with the temporal noise, we find that the value of the DEE remains invariant as shown in Fig. 5. This indicates the robustness of the dynamically generated Floquet Majorana modes against a weak temporal noise in the driving.

VI. DETECTION OF THE ANOMALOUS EDGE MODES WITH PERIODICALLY MODULATED HOPPING PARAMETER THROUGH DEE

We now consider the periodic driving of the hopping parameter γ , which may be complex in general, so that the Hamiltonian in (4) is modified to

$$H(t) = - \sum_{n=1}^{L-1} (\gamma(t) c_n^\dagger c_{n+1} + \gamma^*(t) c_{n+1}^\dagger c_n) - \mu \sum_{n=1}^L (2c_n^\dagger c_n - 1) + \sum_{n=1}^{L-1} \Delta (c_n c_{n+1} + c_{n+1}^\dagger c_n^\dagger). \quad (9)$$

It has been established that for this type of driving protocol, modes localized at the edges with the eigenvalues of the Floquet operator away from ± 1 (referred to as anomalous modes) can dynamically emerge [15]. We address here the question of whether the DEE can detect these anomalous modes.

A. Periodic driving of the amplitude of the hopping parameter

We consider the following form of the hopping parameter,

$$\gamma(t) = \gamma_0 (1 + a \cos(\omega t)), \quad (10)$$

where $\omega = 2\pi/T$, and a determines the strength of the modulation of the hopping amplitude. Since the hopping parameter is chosen to be real, the time-reversal symmetry of the Hamiltonian $H(t)$ is preserved, and the periodically driven chain belongs to the BDI (Floquet) symmetry class.

To see if there are emergent anomalous modes, we plot the Floquet quasienergies θ as a function of ω for $a = 1$ in Fig. 6(a). Evidently, for $1.5 < \omega < 2.0$, the extreme values (near the top and bottom) of the Floquet quasienergies are separated by finite gaps from the other quasienergies. The modes with these isolated values of Floquet quasienergies are known as anomalous modes [15] since the corresponding eigenvalues of the Floquet operator differ from ± 1 .

In Fig. 6(b), the variation of the inverse participation ratio (IPR) is plotted against the real part of the corresponding eigenvalues of the Floquet operator for $\omega = 1.7$. (For a normalized wave function $\psi_j(n)$, where j labels the wave function and n denotes the site index, the IPR is defined as $\sum_n |\psi_j(n)|^4$. It is known that as the system size L is taken to infinity, the IPRs of modes which are extended in the bulk go to zero while the IPRs of modes localized at the ends remain finite. Hence a plot of the IPR versus j provides an easy way to identify the edge modes). From this figure, it can clearly be seen that the anomalous modes [which have the minimum real part (not equal to -1) of the eigenvalues of the Floquet operator] have relatively large IPRs, compared to the other

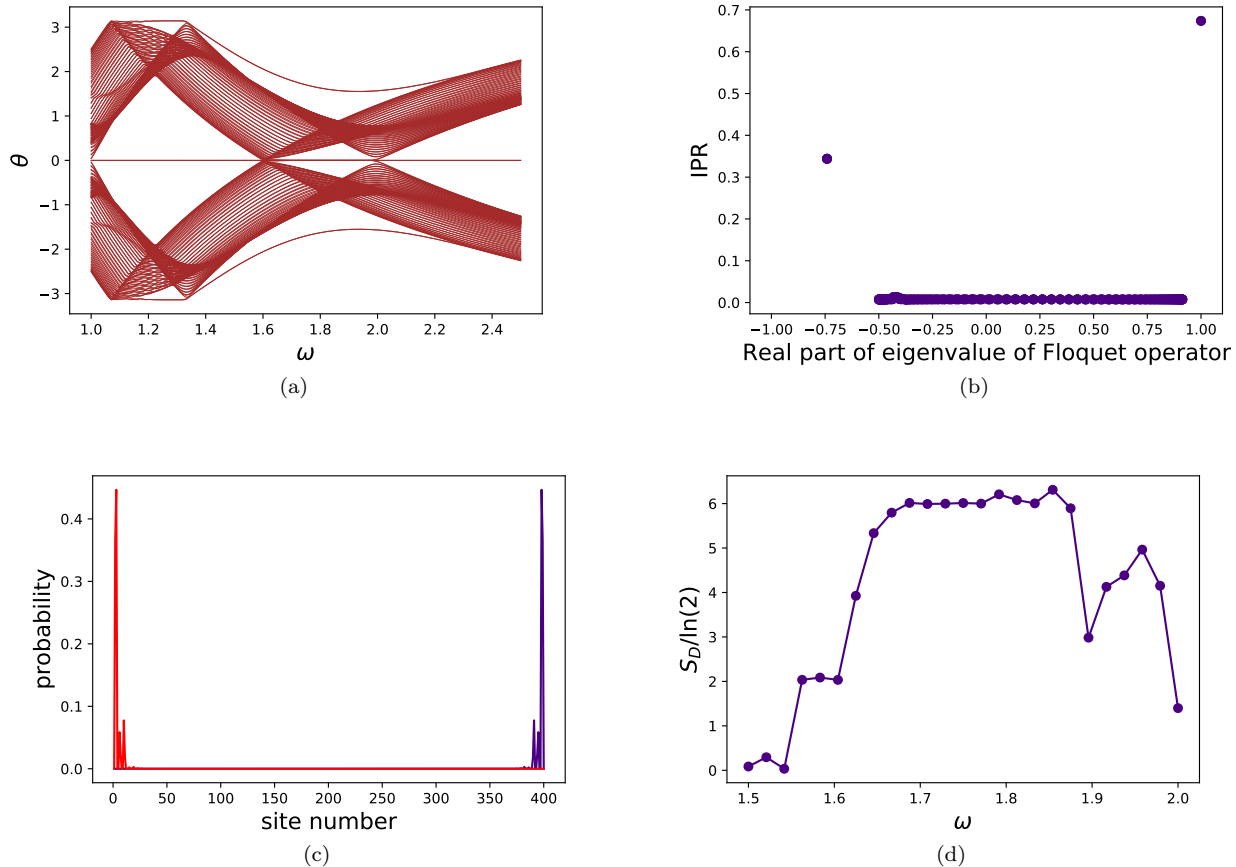


FIG. 6. (a) Floquet quasienergies θ as a function of the drive frequency ω (the two isolated lines seen near the top and bottom in the frequency range of about $[1.4, 2.2]$ correspond to anomalous end modes. The two isolated lines seen near the top and bottom in the frequency range of about $[1.1, 1.4]$ correspond to Majorana π modes.) (b) Inverse participation ratio (IPR) as a function of the real part of the eigenvalue of the Floquet operator (U_F) at $\omega = 1.6$ and for $L = 200$. The modes with the real part of eigenvalue $+1$ of the Floquet operator are Majorana zero modes and the modes with the minimum real part of eigenvalue (if it is not equal to -1) of the Floquet operator are anomalous modes. There are four anomalous modes and two zero-energy modes. (c) Probability as a function of the site number for two anomalous modes with the eigenvalues $-0.7412 \pm 0.6713i$ of the Floquet operator U_F at $\omega = 1.6$. (d) DEE (S_D) in units of $\ln(2)$ as a function of ω for $L = 400$ and $L_D = 100$. For all the plots, the amplitude of the hopping parameter is periodically modulated (see Eq. (10)) with $a = 1.0$. We have taken $\mu = 0$, $\Delta = 0.8$ and $\gamma_0 = 1.0$.

modes having non-zero Floquet quasienergies. We note here that the IPRs of the anomalous modes are almost comparable to that of the zero-energy Majorana modes (with the eigenvalue of the Floquet operator being equal to $+1$). Fig. 6(c) further confirms that these anomalous modes, despite having non-zero Floquet quasienergies, are localized at the edges of the chain [15].

In Fig. 6(d), the DEE (S_D) is plotted as a function of the drive frequency ω to find the contribution of both the anomalous modes and the zero-energy modes to the DEE. As is evident from Fig. 6(d), in the approximate range of frequencies between $[1.6, 1.8]$, the non-zero and integer-quantized contribution of the anomalous modes and the zero-energy modes to the DEE enables us to detect these edge modes. In this range of frequencies, there are four anomalous modes and two Floquet zero-energy

Majorana modes (two zero-energy Majorana modes are generated at $\omega = 2$ for $\gamma_0 = 1$, as can be seen from the analytical calculation provided in Appendix E) and the DEE is nearly equal to $6 \ln(2)$. Thus, we observe that $S_D/\ln(2)$ matches exactly with the total number of edge modes (the zero-energy Majorana modes as well as the anomalous modes) for $1.6 \lesssim \omega \lesssim 1.8$. In this range of frequency, the DEE is able to detect the anomalous modes and zero-energy Majorana modes. Subsequently, we will illustrate in Sec. VIC that the zero-energy Floquet Majorana modes are robust against weak spatial disorder while the anomalous modes are not.

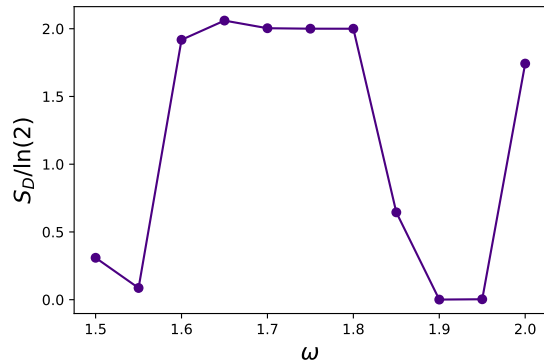


FIG. 7. DEE (S_D) in units of $\ln(2)$ as a function of drive-frequency (ω) for periodic driving of the amplitude of the hopping parameter in the presence of spatial disorder (see Eq. (12)). We have taken $L = 200$, $L_D = 50$, $\Delta = 0.8$, $\mu = 0$, $\gamma_0 = 1.0$ and $a = 1.0$. For this protocol, ν_n assumes a random value in the range $[0, 1]$ at each site n . The DEE has been calculated after taking the average over a large number of configurations of random numbers.

B. Periodic driving of the phase of the complex hopping parameter

Now we consider the hopping parameter to be complex [15], with the form

$$\gamma(t) = \gamma_0 \exp[ia \cos(\omega t)], \quad (11)$$

where $\omega = 2\pi/T$, and the parameter a determines the strength of the modulation of the phase of the hopping parameter. The complex hopping parameter in Eq. (11) explicitly breaks the time-reversal symmetry of the Hamiltonian $H(t)$ [12, 15]. Therefore, a chain periodically driven with this protocol belongs to the D (Floquet) symmetry class. For this driving protocol, similar to the protocol discussed in Sec. VIA, zero-energy Floquet Majorana modes and anomalous modes appear. However, we find that the DEE, calculated using the methods provided in Appendix B, is not able to count the anomalous edge modes and zero-energy Majorana modes correctly for this driving protocol.

C. Effect of spatial disorder on the DEE for periodic driving of hopping parameter

In this section, we investigate whether the dynamical zero-energy Majorana modes and the anomalous modes discussed in Sec. VIA survive in the presence of weak spatial disorder. To this end, we explore the effects of disorder on the DEE for a periodic driving of the nearest-neighbor hopping amplitude.

Let us consider the driving protocol where the amplitude of the nearest-neighbor hopping parameter $\gamma_n(t)$ for the n -th site is periodically modulated in the presence

of spatial disorder. Therefore, this is the same driving protocol as in Eq. (10), but in the presence of spatial disorder. For this driving protocol, $\gamma_n(t)$ is given by,

$$\gamma_n(t) = \gamma_0(1 + a\nu_n \cos(\omega t)), \quad (12)$$

where γ_0 and the modulation strength a are independent of site index n , and ν_n assumes random value in the range $[0, 1]$ for each site n . From Fig. 7, it can clearly be seen that for $1.6 \lesssim \omega \lesssim 1.8$, the DEE is almost constant and equal to $2 \ln(2)$ in the presence of spatial disorder. On the other hand, in the absence of disorder, the DEE is equal to $6 \ln(2)$ (as there are four anomalous modes and two zero-energy modes) in the same range of ω (see Fig. 6(d)). From this observation, we infer that the two zero-energy modes remain robust against spatial disorder, whereas the four anomalous edge modes disappear in the presence of spatial disorder.

VII. CONCLUSIONS

In this paper, we have shown that for the periodic driving protocol of the chemical potential, the DEE, calculated in the ground state of the Floquet Hamiltonian, is integer-quantized, with the integer being equal to the total number of dynamically generated Floquet Majorana edge modes. Thus, it can be inferred that similar to the static situation, the DEE can act as a marker of Majorana edge modes even for a periodically driven Kitaev chain. At low frequencies, there is an apparent discrepancy and the value of $S_D/\ln(2)$ differs significantly from the number of Majorana end modes. However, this is an artefact of the finite size of the system, and we have established that the DEE saturates to an integer-quantized value at large system size L , even at low drive frequencies (ω of the order of the hopping amplitude γ). Thus, in a periodically driven chain with open boundary conditions, the DEE counts the number of edge Majorana modes correctly and therefore plays a role similar to that played by the winding number derived from the Floquet Hamiltonian in the corresponding system with periodic boundary conditions.

If the amplitude of the nearest-neighbor hopping in the Kitaev chain is periodically modulated (see the protocol in Eq. (10)), such that the Floquet Hamiltonian remains in the BDI symmetry class, then “anomalous” edge modes (with Floquet quasienergies not equal to zero or π) can be dynamically generated. Although these anomalous edge modes do not have a topological origin and are not associated with a winding number, we find that the DEE is able to detect the existence of the anomalous edge modes for certain ranges of driving frequencies. Furthermore, we illustrate that the anomalous edge modes are not robust against weak spatial disorder, and they disappear in that situation while the zero-energy Majorana modes survive.

The dynamical generation of anomalous edge modes is also possible with the periodic modulation of the phase of the complex hopping parameter (see the driving protocol in Eq. (11), where the system belongs to Floquet D symmetry class). However, for this driving protocol, the DEE fails to detect them properly. Further, we have checked that one cannot infer conclusively the effects of disorder on both zero-energy and anomalous modes in the presence of spatial disorder. Why the DEE fails to detect edge modes of both types when the Floquet Hamiltonian is in the symmetry class D is an unresolved question at the moment that requires further investigation.

We conclude by noting that recently the topological entanglement entropy has been measured experimentally for a two-dimensional toric code model [65]; the quantity has been measured experimentally using simulated anyon interferometry and extracting the braiding statistics of emergent excitation [65]. On the other hand, in the present work, we have computed the DEE for one-dimensional Kitaev model where anyons do not exist. We are also not aware of an equivalent of the DEE in two-dimensional situations. This experiment however provides a motivation for an experimental measurement of the DEE for one-dimensional topological systems and a possible generalization of the DEE for two-dimensional systems.

In conclusion, we note that it would be interesting to investigate out-of-equilibrium behavior of the DEE in Kitaev chains with more complicated interactions, like next-nearest-neighbor hopping and superconducting pairing [12, 66].

ACKNOWLEDGMENTS

S.M. acknowledges financial support from PMRF fellowship, MHRD, India. D.S. thanks SERB, India for funding through Project No. JBR/2020/000043. A.D. acknowledges support from SPARC program, MHRD, India and SERB, DST, New Delhi, India. We acknowledge Souvik Bandyopadhyay and Sourav Bhattacharjee for comments.

Appendix A: Winding number and topological properties of short-range Kitaev chain

The Hamiltonian H in Eq. (4) of a short-range Kitaev chain with periodic boundary conditions can be written in terms of the fermionic creation and annihilation operators in momentum space as

$$H = \sum_k (c_k^\dagger \ c_{-k}) H_k \begin{pmatrix} c_k \\ c_{-k}^\dagger \end{pmatrix}, \quad (\text{A1})$$

where k lies in the range $[-\pi, \pi]$, and the Hamiltonian H_k is given by

$$H_k = (-\gamma \cos k - \mu) \sigma_z + \Delta \sin k \sigma_y, \quad (\text{A2})$$

where σ_y and σ_z are Pauli matrices. In the ground state of the Hamiltonian H in Eq. (4), the winding number [11] is defined as

$$w = \frac{1}{2\pi} \int_{-\pi}^{\pi} dk \frac{d\phi_k}{dk}, \quad (\text{A3})$$

$$\phi_k = \tan^{-1} \left(\frac{\Delta \sin k}{\gamma \cos k + \mu} \right). \quad (\text{A4})$$

Setting the hopping parameter $\gamma = 1$, it is straightforward to check that the following phases exist in the ground state of a short-range Kitaev chain (in static situation).

1. Topologically non-trivial phase ($-1 < \mu < 1$): This phase consists of phase I ($\Delta > 0$) and phase II ($\Delta < 0$). The winding numbers in phases I and phases II are given by $w = +1$ and $w = -1$, respectively [11]. For a chain with open boundary condition, these topologically non-trivial phases are characterized by the existence of a zero-energy Majorana mode localized at each edge of the chain [11].
2. Topologically trivial phase ($|\mu| > 1$): The winding number is zero ($w = 0$) in this phase. For a chain with open boundary condition, Majorana edge modes do not appear in this phase.

Appendix B: Methods used for calculation of the DEE from Floquet Hamiltonian

Each fermionic creation operator c_n^\dagger (or annihilation operator c_n) can be written as a linear combination of two Hermitian Majorana operators (a_{2n-1} and a_{2n}) as

$$c_n = \frac{1}{2}(a_{2n-1} - ia_{2n}), \quad (\text{B1a})$$

$$c_n^\dagger = \frac{1}{2}(a_{2n-1} + ia_{2n}). \quad (\text{B1b})$$

The Hamiltonian $H(t)$ of a Kitaev chain with generic time-dependent parameters can be written as,

$$H(t) = i \sum_{m=1}^{2L} \sum_{n=1}^{2L} a_m M_{mn}(t) a_n, \quad (\text{B2})$$

where $M(t)$ is a $2L \times 2L$ real, antisymmetric matrix (which follows from the fact that Majorana operators satisfy anticommutation relations: $\{a_m, a_n\} = 2\delta_{mn}$). The $2L \times 1$ column matrix of the Majorana operators $a(t) = (a_1(t) \ a_2(t) \ \dots \ a_{2L}(t))^T$ in Heisenberg picture can be written as,

$$a(t) = \mathbb{T} \exp \left(4 \int_0^t M(t') dt' \right) a(0) = U(t) a(0). \quad (\text{B3})$$

Thus, the stroboscopic time-evolution operator (Floquet operator) is given by,

$$U_F = U(T) = \mathbb{T} \exp\left(4 \int_0^T M(t') dt'\right). \quad (\text{B4})$$

As U_F is unitary matrix, each of its eigenvalues λ satisfies the property $|\lambda| = 1$. Thus, λ must be phases. Further, the matrix U_F is real, which ensures that the eigenvalues of U_F must appear in complex conjugate pairs, i.e., $e^{i\theta}$ and $e^{-i\theta}$.

In the ground state of the Floquet Hamiltonian H_F (where $U_F = \exp(-iH_F T)$), all the negative quasienergy eigenstates (the L eigenstates with the lowest quasienergies) are filled and all the positive quasienergy eigenstates (the L eigenstates with the highest quasienergies) are empty. For a subsystem X with L_X fermionic sites, an element of the $2L_X \times 2L_X$ correlation matrix A_X in the Majorana basis, calculated in the ground state of the Floquet Hamiltonian, can be written as

$$(A_X)_{mn} = \langle a_m a_n \rangle = \sum_{j=1}^L \langle \psi_j | a_m a_n | \psi_j \rangle, \quad (\text{B5})$$

where $|\psi_j\rangle$ is an eigenstate of the Floquet Hamiltonian H_F , and the index j denotes the ascending order of Floquet quasienergy. The von Neumann entropy S_X of the subsystem X is obtained from the eigenvalues α_j of the correlation matrix A_X as

$$S_X = - \sum_{j=1}^{2L_X} \alpha_j \ln(\alpha_j). \quad (\text{B6})$$

S_X for $X = A, B, A \cap B$ and $A \cup B$ are calculated in the ground state of Floquet Hamiltonian and the DEE is then computed using Eq. (3).

Appendix C: DEE for a Kitaev chain with chemical potential periodically modulated with square pulse and sinusoidal variation

Let the chemical potential μ be periodically modulated by square pulses of the symmetrized form (i.e., $\mu(t) = \mu(T - t)$), which ensures that $\sigma_x H_k(t) \sigma_x = -H_k(T - t)$)

$$\mu(t) = \begin{cases} \mu_0 + \mu_1 & \text{for } 0 < t < \frac{T}{4}, \\ \mu_0 - \mu_1 & \text{for } \frac{T}{4} < t < \frac{3T}{4}, \\ \mu_0 + \mu_1 & \text{for } \frac{3T}{4} < t < T, \end{cases} \quad (\text{C1})$$

where $T = 2\pi/\omega$. From Fig. 8, we observe that the value of $S_D/\ln(2)$ is integer-quantized and is equal to total number p of Majorana edge modes generated by the same square pulse, unless the drive frequency is sufficiently small. We reiterate that the discrepancy in the value of $S_D/\ln(2)$ at low drive frequencies occurs due to the finiteness of the system size L .

Finally, for a sinusoidal variation of μ of the form

$$\mu(t) = \mu_0 + \mu_1 \cos(\omega t), \quad (\text{C2})$$

we obtain similar results for the DEE as shown in Fig. 9. Note that the driving satisfies $\mu(t) = \mu(T - t)$.

Appendix D: Comparison of the DEE with the dynamical winding number for periodically driven Kitaev chain

In this section, we compare the results inferred from the behavior of the DEE with the dynamical winding number for driving protocols discussed in Sec. IV.

For a periodically driven Kitaev chain with periodic boundary conditions, the winding number may be calculated from the stroboscopic time-evolution operator (i.e., Floquet operator)

$$U_F(k) = \mathbb{T} \exp\left(-i \int_0^T H_k(t) dt\right) = \exp(-ih_k^F T), \quad (\text{D1})$$

for momentum $k \in [-\pi, \pi]$, where h_k^F and $H_k(t)$ are, respectively, the Floquet Hamiltonian and the instantaneous Hamiltonian for the mode with momentum k . Referring to Eq. (A2), for a generic time-dependent chemical potential, we get

$$H_k(t) = (-\gamma \cos k - \mu(t)) \sigma_z + \Delta \sin k \sigma_y. \quad (\text{D2})$$

On the other hand, for a periodic driving, the general form of the Floquet Hamiltonian h_k^F can be written as

$$h_k^F = d_0(k) \mathbb{1} + d_x(k) \sigma_x + d_y(k) \sigma_y + d_z(k) \sigma_z, \quad (\text{D3})$$

where $\sigma_x, \sigma_y, \sigma_z$ are Pauli matrices and $\mathbb{1}$ is 2×2 identity matrix. Since $U_F(k)$ is a $SU(2)$ matrix (due to the fact that $H_k(t)$ can be written as the sum of Pauli matrices with appropriate coefficients), we have $d_0(k) = 0$ for all values of $k \in [-\pi, \pi]$. Thus, the Floquet Hamiltonian h_k^F [11, 15] reduces to the form

$$h_k^F = d_x(k) \sigma_x + d_y(k) \sigma_y + d_z(k) \sigma_z. \quad (\text{D4})$$

The coefficients d_x, d_y and d_z assume different forms for different driving protocols.

If the chemical potential is periodically modulated with δ -pulses (Eq. (6)), the symmetrized Floquet operator $U_F(k)$ is given by

$$U_F(k) = e^{i\frac{\mu_1}{2}\sigma_z} e^{-iT[(-\gamma \cos k - \mu_0) \sigma_z + \Delta \sin k \sigma_y]} e^{i\frac{\mu_1}{2}\sigma_z}. \quad (\text{D5})$$

Since we have chosen the driving to satisfy $\mu(t) = \mu(T - t)$ and $\sigma_x H_k(t) \sigma_x = -H_k(T - t)$, we see that $\sigma_x U_F(k) \sigma_x = [U_F(k)]^\dagger$ for all $k \in [-\pi, \pi]$. Using $U_F(k) = \exp(-ih_k^F T)$ and Eq. (D4), we find that $d_x(k) = 0$; we can see in Fig. 10(a) that this is true. We then arrive at a simplified form of the Floquet Hamiltonian h_k^F

$$h_k^F = d_y(k) \sigma_y + d_z(k) \sigma_z. \quad (\text{D6})$$

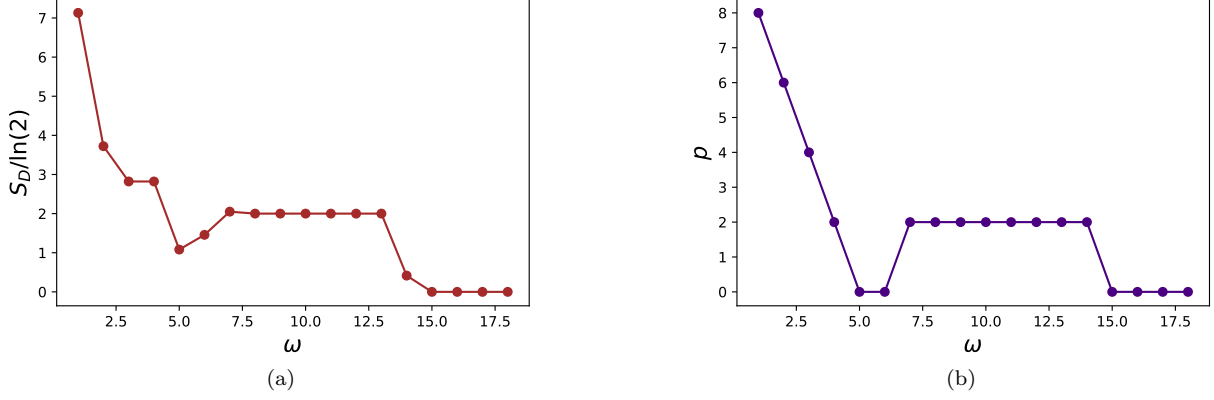


FIG. 8. (a) DEE (S_D) in units of $\ln(2)$ and (b) total number of Majorana edge modes p as functions of ω for a Kitaev chain in which the chemical potential μ is periodically modulated by a square pulse (Eq. (C1)) having $\mu_0 = 2.5$ and $\mu_1 = 0.2$. We have taken $L = 200$ and $L_D = 50$.

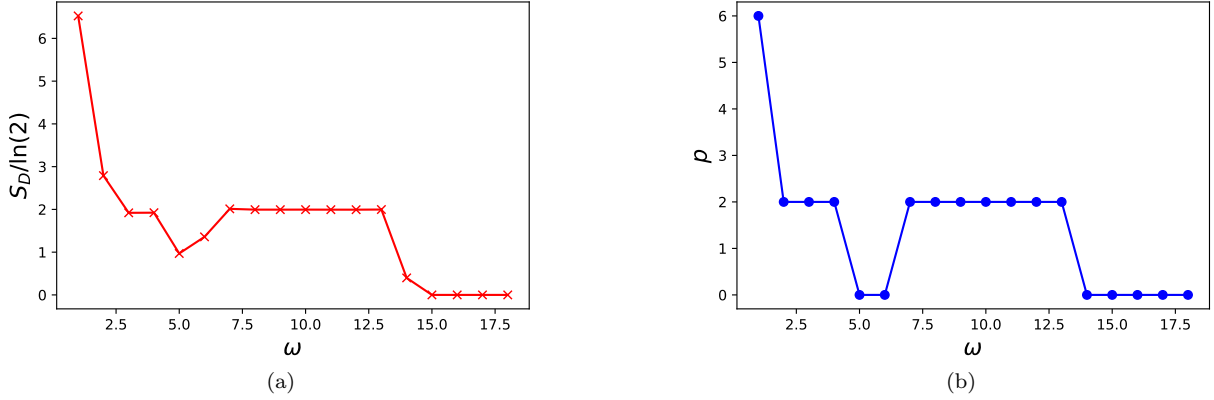


FIG. 9. (a) DEE (S_D) in units of $\ln(2)$ and (b) total number of Majorana edge modes p as functions of ω for a Kitaev chain in which the chemical potential μ is periodically driven with sinusoidal modulation (Eq. (C2)) having $\mu_0 = 2.5$, $\mu_1 = 0.2$. We have taken $L = 200$ and $L_D = 50$.

This particular form of h_k^F enables us to define a dynamical winding number [11] in the following way: $d_z(k)$ is plotted as a function of $d_y(k)$ (see Figs. 10(b), 10(c) and 10(d)) and the number of times the curve winds around the origin (located at $d_y = 0$, $d_z = 0$) is counted. This gives the value of the winding number, which turns out to be equal to the number of zero-energy Majorana modes at each end of an open chain. Thus, the winding number is able to characterize the topology of the Kitaev chain periodically driven with a δ -pulse. On the other hand, the DEE, which can assume any real value, turns out to be an integer multiple of $\ln(2)$ (see Fig. 2). The equivalence of the DEE with the winding number in detecting the Majorana edge modes for the periodic modulation with a δ -pulse is thus established.

Now, for periodic driving with square pulse (Eq. (C1)) and sinusoidal variation (Eq. (C2)), where we have again chosen a symmetrized form of the chemical potential

(i.e., $\mu(t) = \mu(T - t)$), a similar argument shows that $d_x(k) = 0$ for all $k \in [-\pi, \pi]$. Thus, the corresponding Floquet Hamiltonian h_k^F can be written as Eq. (D6), and we can derive the dynamical winding number from the Floquet Hamiltonian. Proceeding in a similar way as done for the periodic driving with δ -pulses, the equivalence of the winding number and the DEE can be established.

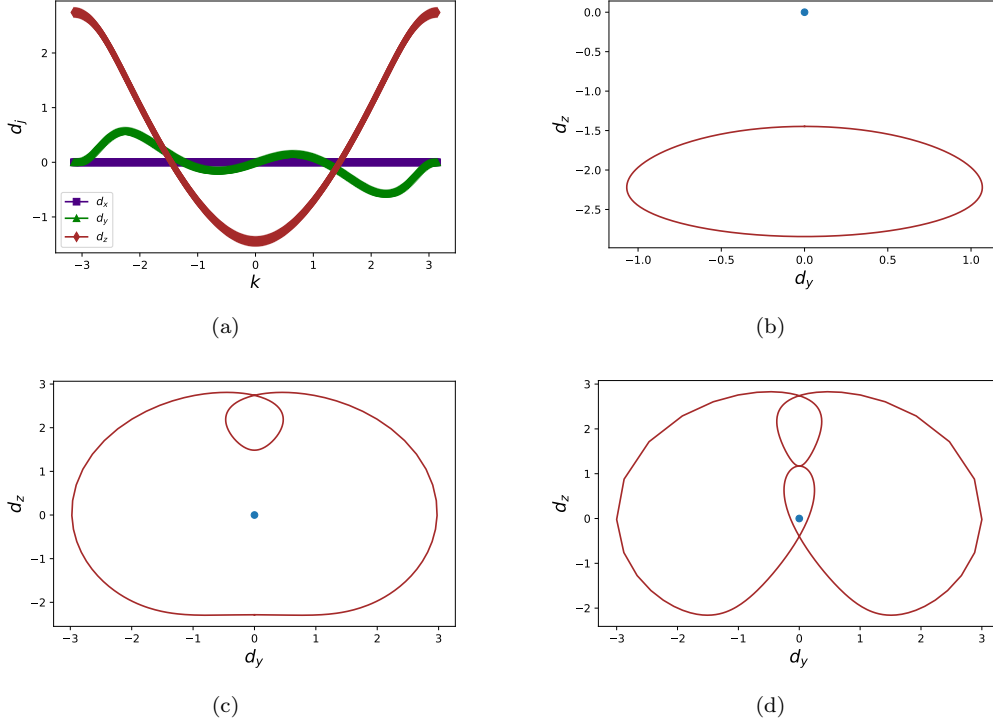


FIG. 10. (a) d_x , d_y and d_z as functions of k for periodic driving of the chemical potential with a δ -pulse having $\mu_0 = 2.5$, $\mu_1 = 0.2$, and $\omega = 6.0$. We find that $d_x = 0$ for all values of k . (b) d_z as a function of d_y for $\omega = 18.0$. The dynamical (Floquet) winding number is zero. (c) d_z as a function of d_y for $\omega = 10.0$. The winding number is 1. (d) d_z as a function of d_y for $\omega = 4.0$. The winding number is 2.

Appendix E: Closing of Floquet quasienergy gap for periodic driving of hopping parameter

The Floquet operator for the mode with momentum $k \in [0, \pi]$ is given by

$$U_F(k) = \mathbb{T} \exp\left(-i \int_0^T H_k(t) dt\right) = \exp(-ih_k^F T), \quad (\text{E1})$$

where h_k^F is the corresponding Floquet Hamiltonian. For a time-dependent hopping amplitude $\gamma(t)$, $H_k(t)$ for $k \in [0, \pi]$ has the form

$$H_k(t) = (-2\gamma(t) \cos k - 2\mu) \sigma_z + 2\Delta \sin k \sigma_y, \quad (\text{E2})$$

where $\gamma(t) = \gamma_0(1 + a \cos(\omega t))$ (see Eq. (10)). Using Eq. (E1), we obtain the following two equations for $k = 0$ and $k = \pi$, respectively:

$$U_F(k = 0) = \exp(2iT(\gamma_0 + \mu)), \quad (\text{E3a})$$

$$U_F(k = \pi) = \exp(-2iT(\gamma_0 - \mu)). \quad (\text{E3b})$$

For $\mu = 0$, the condition $U_F(k = 0) = U_F(k = \pi) = \mathbb{1}$ is satisfied at the drive frequency $\omega = 2\gamma_0/q$, where q is a positive integer. At these frequencies, the Floquet quasienergy gap closes. Thus, the generation of zero-energy Floquet Majorana modes occurs at these specific frequencies for the driving protocol given in Eq. (10). For the periodic driving of the chemical potential, an analytical derivation of the frequencies at which the Floquet quasienergy gap closes can also be done by proceeding in the same way as discussed in this section (See Ref. [11]).

- [1] M. Z. Hasan and C. L. Kane, Colloquium: Topological insulators, *Rev. Mod. Phys.* **82**, 3045 (2010).
 [2] X.-L. Qi and S.-C. Zhang, Topological insulators and superconductors, *Rev. Mod. Phys.* **83**, 1057 (2011).

- [3] L. Fidkowski and A. Kitaev, Topological phases of fermions in one dimension, *Phys. Rev. B* **83**, 075103 (2011).
 [4] X. Chen, Z.-C. Gu, Z.-X. Liu, and X.-G. Wen, Symmetry protected topological orders and the group cohomology of

- their symmetry group, Phys. Rev. B **87**, 155114 (2013).
- [5] T. Senthil, Symmetry-protected topological phases of quantum matter, Annual Review of Condensed Matter Physics **6**, 299 (2015), <https://doi.org/10.1146/annurev-conmatphys-031214-014740>.
- [6] C.-K. Chiu, J. C. Y. Teo, A. P. Schnyder, and S. Ryu, Classification of topological quantum matter with symmetries, Rev. Mod. Phys. **88**, 035005 (2016).
- [7] A. Y. Kitaev, Unpaired majorana fermions in quantum wires, Physics-Uspekhi **44**, 131 (2001).
- [8] A. Kitaev and C. Laumann, Topological phases and quantum computation 10.48550/arxiv.0904.2771 (2009).
- [9] W. DeGottardi, D. Sen, and S. Vishveshwara, Topological phases, majorana modes and quench dynamics in a spin ladder system, New Journal of Physics **13**, 065028 (2011).
- [10] W. DeGottardi, D. Sen, and S. Vishveshwara, Majorana fermions in superconducting 1d systems having periodic, quasiperiodic, and disordered potentials, Phys. Rev. Lett. **110**, 146404 (2013).
- [11] M. Thakurathi, A. A. Patel, D. Sen, and A. Dutta, Floquet generation of majorana end modes and topological invariants, Phys. Rev. B **88**, 155133 (2013).
- [12] W. DeGottardi, M. Thakurathi, S. Vishveshwara, and D. Sen, Majorana fermions in superconducting wires: Effects of long-range hopping, broken time-reversal symmetry, and potential landscapes, Phys. Rev. B **88**, 165111 (2013).
- [13] A. Rajak and A. Dutta, Survival probability of an edge majorana in a one-dimensional p -wave superconducting chain under sudden quenching of parameters, Phys. Rev. E **89**, 042125 (2014).
- [14] A. Dutta, G. Aeppli, B. K. Chakrabarti, U. Divakaran, T. F. Rosenbaum, and D. Sen, *Quantum Phase Transitions in Transverse Field Spin Models: From Statistical Physics to Quantum Information* (Cambridge University Press, 2015).
- [15] S. Saha, S. N. Sivarajan, and D. Sen, Generating end modes in a superconducting wire by periodic driving of the hopping, Phys. Rev. B **95**, 174306 (2017).
- [16] S. Bandyopadhyay, S. Bhattacharjee, and A. Dutta, Dynamical generation of majorana edge correlations in a ramped kitaev chain coupled to nonthermal dissipative channels, Phys. Rev. B **101**, 104307 (2020).
- [17] S. Bandyopadhyay, S. Bhattacharjee, and D. Sen, Driven quantum many-body systems and out-of-equilibrium topology, Journal of Physics: Condensed Matter **33**, 393001 (2021).
- [18] A. Russomanno, A. Silva, and G. E. Santoro, Periodic steady regime and interference in a periodically driven quantum system, Phys. Rev. Lett. **109**, 257201 (2012).
- [19] M. Tomka, A. Polkovnikov, and V. Gritsev, Geometric phase contribution to quantum nonequilibrium many-body dynamics, Phys. Rev. Lett. **108**, 080404 (2012).
- [20] T. Nag, S. Roy, A. Dutta, and D. Sen, Dynamical localization in a chain of hard core bosons under periodic driving, Phys. Rev. B **89**, 165425 (2014).
- [21] M. Bukov, L. D'Alessio, and A. Polkovnikov, Universal high-frequency behavior of periodically driven systems: from dynamical stabilization to floquet engineering, Advances in Physics **64**, 139 (2015), <https://doi.org/10.1080/00018732.2015.1055918>.
- [22] S. Dasgupta, U. Bhattacharya, and A. Dutta, Phase transition in the periodically pulsed dicke model, Phys. Rev. E **91**, 052129 (2015).
- [23] T. Nag, D. Sen, and A. Dutta, Maximum group velocity in a one-dimensional model with a sinusoidally varying staggered potential, Phys. Rev. A **91**, 063607 (2015).
- [24] A. Sen, S. Nandy, and K. Sengupta, Entanglement generation in periodically driven integrable systems: Dynamical phase transitions and steady state, Phys. Rev. B **94**, 214301 (2016).
- [25] B. Mukherjee, A. Sen, D. Sen, and K. Sengupta, Signatures and conditions for phase band crossings in periodically driven integrable systems, Phys. Rev. B **94**, 155122 (2016).
- [26] A. Eckardt, Colloquium: Atomic quantum gases in periodically driven optical lattices, Rev. Mod. Phys. **89**, 011004 (2017).
- [27] T. Oka and S. Kitamura, Floquet engineering of quantum materials, Annual Review of Condensed Matter Physics **10**, 387 (2019), <https://doi.org/10.1146/annurev-conmatphys-031218-013423>.
- [28] A. Sen, D. Sen, and K. Sengupta, Analytic approaches to periodically driven closed quantum systems: methods and applications, Journal of Physics: Condensed Matter **33**, 443003 (2021).
- [29] T. Kitagawa, E. Berg, M. Rudner, and E. Demler, Topological characterization of periodically driven quantum systems, Phys. Rev. B **82**, 235114 (2010).
- [30] L. Jiang, T. Kitagawa, J. Alicea, A. R. Akhmerov, D. Pekker, G. Refael, J. I. Cirac, E. Demler, M. D. Lukin, and P. Zoller, Majorana fermions in equilibrium and in driven cold-atom quantum wires, Phys. Rev. Lett. **106**, 220402 (2011).
- [31] Z. Gu, H. A. Fertig, D. P. Arovas, and A. Auerbach, Floquet spectrum and transport through an irradiated graphene ribbon, Phys. Rev. Lett. **107**, 216601 (2011).
- [32] M. Trif and Y. Tserkovnyak, Resonantly tunable majorana polariton in a microwave cavity, Phys. Rev. Lett. **109**, 257002 (2012).
- [33] D. E. Liu, A. Levchenko, and H. U. Baranger, Floquet majorana fermions for topological qubits in superconducting devices and cold-atom systems, Phys. Rev. Lett. **111**, 047002 (2013).
- [34] A. Kundu and B. Seradjeh, Transport signatures of floquet majorana fermions in driven topological superconductors, Phys. Rev. Lett. **111**, 136402 (2013).
- [35] C. C. Wu, J. Sun, F. J. Huang, Y. D. Li, and W. M. Liu, Majorana fermions in a periodically driven semiconductor-superconductor heterostructure, EPL (Europhysics Letters) **104**, 27004 (2013).
- [36] Q.-J. Tong, J.-H. An, J. Gong, H.-G. Luo, and C. H. Oh, Generating many majorana modes via periodic driving: A superconductor model, Phys. Rev. B **87**, 201109 (2013).
- [37] A. A. Reynoso and D. Frustaglia, Unpaired floquet majorana fermions without magnetic fields, Phys. Rev. B **87**, 115420 (2013).
- [38] N. H. Lindner, D. L. Bergman, G. Refael, and V. Galitski, Topological floquet spectrum in three dimensions via a two-photon resonance, Phys. Rev. B **87**, 235131 (2013).
- [39] Y. T. Katan and D. Podolsky, Modulated floquet topological insulators, Phys. Rev. Lett. **110**, 016802 (2013).
- [40] M. Thakurathi, K. Sengupta, and D. Sen, Majorana edge modes in the kitaev model, Phys. Rev. B **89**, 235434 (2014).

- [41] J. K. Asbóth, B. Tarasinski, and P. Delplace, Chiral symmetry and bulk-boundary correspondence in periodically driven one-dimensional systems, *Phys. Rev. B* **90**, 125143 (2014).
- [42] M. D. Reichl and E. J. Mueller, Floquet edge states with ultracold atoms, *Phys. Rev. A* **89**, 063628 (2014).
- [43] P. M. Perez-Piskunow, L. E. F. Foa Torres, and G. Usaj, Hierarchy of floquet gaps and edge states for driven honeycomb lattices, *Phys. Rev. A* **91**, 043625 (2015).
- [44] A. Agarwala, U. Bhattacharya, A. Dutta, and D. Sen, Effects of periodic kicking on dispersion and wave packet dynamics in graphene, *Phys. Rev. B* **93**, 174301 (2016).
- [45] R. Roy and F. Harper, Abelian floquet symmetry-protected topological phases in one dimension, *Phys. Rev. B* **94**, 125105 (2016).
- [46] S. Yao, Z. Yan, and Z. Wang, Topological invariants of floquet systems: General formulation, special properties, and floquet topological defects, *Phys. Rev. B* **96**, 195303 (2017).
- [47] M. Thakurathi, D. Loss, and J. Klinovaja, Floquet majorana fermions and parafermions in driven rashba nanowires, *Phys. Rev. B* **95**, 155407 (2017).
- [48] M. Rodriguez-Vega and B. Seradjeh, Universal fluctuations of floquet topological invariants at low frequencies, *Phys. Rev. Lett.* **121**, 036402 (2018).
- [49] T. Čadež, R. Mondaini, and P. D. Sacramento, Edge and bulk localization of floquet topological superconductors, *Phys. Rev. B* **99**, 014301 (2019).
- [50] U. Bhattacharya, S. Maity, A. Dutta, and D. Sen, Critical phase boundaries of static and periodically kicked long-range kitaev chain, *Journal of Physics: Condensed Matter* **31**, 174003 (2019).
- [51] G. Floquet, Sur les équations différentielles linéaires à coefficients périodiques, *Annales scientifiques de l'École Normale Supérieure* **2e série**, **12**, 47 (1883).
- [52] M. McGinley and N. R. Cooper, Topology of one-dimensional quantum systems out of equilibrium, *Phys. Rev. Lett.* **121**, 090401 (2018).
- [53] S. Bandyopadhyay, U. Bhattacharya, and A. Dutta, Temporal variation in the winding number due to dynamical symmetry breaking and associated transport in a driven su-schrieffer-heeger chain, *Phys. Rev. B* **100**, 054305 (2019).
- [54] S. Bandyopadhyay and A. Dutta, Dynamical preparation of a topological state and out-of-equilibrium bulk-boundary correspondence in a su-schrieffer-heeger chain under periodic driving, *Phys. Rev. B* **100**, 144302 (2019).
- [55] P. Fromholz, G. Magnifico, V. Vitale, T. Mendes-Santos, and M. Dalmonte, Entanglement topological invariants for one-dimensional topological superconductors, *Phys. Rev. B* **101**, 085136 (2020).
- [56] T. Micallo, V. Vitale, M. Dalmonte, and P. Fromholz, Topological entanglement properties of disconnected partitions in the Su-Schrieffer-Heeger model, *SciPost Phys. Core* **3**, 12 (2020).
- [57] S. Mondal, S. Bandyopadhyay, S. Bhattacharjee, and A. Dutta, Detecting topological phase transitions through entanglement between disconnected partitions in a kitaev chain with long-range interactions, *Phys. Rev. B* **105**, 085106 (2022).
- [58] X. Mi, M. Sonner, M. Y. Niu, K. W. Lee, B. Foxen, R. Acharya, I. Aleiner, T. I. Andersen, F. Arute, K. Arya, A. Asfaw, J. Atalaya, R. Babbush, D. Bacon, J. C. Bardin, J. Basso, A. Bengtsson, G. Bortoli, A. Bourassa, L. Brill, M. Broughton, B. B. Buckley, D. A. Buell, B. Burkett, N. Bushnell, Z. Chen, B. Chiaro, R. Collins, P. Conner, W. Courtney, A. L. Crook, D. M. Debroy, S. Demura, A. Dunsworth, D. Eppens, C. Erickson, L. Faoro, E. Farhi, R. Fatemi, L. Flores, E. Forati, A. G. Fowler, W. Giang, C. Gidney, D. Gilboa, M. Giustina, A. G. Dau, J. A. Gross, S. Habegger, M. P. Harrigan, J. Hilton, M. Hoffmann, S. Hong, T. Huang, A. Huff, W. J. Huggins, L. B. Ioffe, S. V. Isakov, J. Iveland, E. Jeffrey, Z. Jiang, C. Jones, D. Kafri, K. Kechedzhi, T. Khattar, S. Kim, A. Kitaev, P. V. Klimov, A. R. Klots, A. N. Korotkov, F. Kostritsa, J. M. Kreikebaum, D. Landhuis, P. Laptev, K.-M. Lau, J. Lee, L. Laws, W. Liu, A. Locharla, E. Lucero, O. Martin, J. R. McClean, M. McEwen, B. M. Costa, K. C. Miao, M. Mohseni, S. Montazeri, A. Morvan, E. Mount, W. Mruczkiewicz, O. Naaman, M. Neeley, C. Neill, M. Newman, T. E. O'Brien, A. Opremcak, A. Petukhov, R. Potter, C. Quintana, N. C. Rubin, N. Saei, D. Sank, K. Sankaragomathi, K. J. Satzinger, C. Schuster, M. J. Shearn, V. Shvarts, D. Strain, Y. Su, M. Szalay, G. Vidal, B. Villalonga, C. Vollgraf-Heidweiller, T. White, Z. J. Yao, P. Yeh, J. Yoo, A. Zalcman, Y. Zhang, N. Zhu, H. Neven, S. Boixo, A. Megrant, Y. Chen, J. Kelly, V. Smelyanskiy, D. A. Abanin, and P. Roushan, Noise-resilient majorana edge modes on a chain of superconducting qubits (2022).
- [59] E. Lieb, T. Schultz, and D. Mattis, Two soluble models of an antiferromagnetic chain, *Annals of Physics* **16**, 407 (1961).
- [60] I. Peschel, Calculation of reduced density matrices from correlation functions, *Journal of Physics A: Mathematical and General* **36**, L205 (2003).
- [61] G. Vidal, J. I. Latorre, E. Rico, and A. Kitaev, Entanglement in quantum critical phenomena, *Phys. Rev. Lett.* **90**, 227902 (2003).
- [62] P. Calabrese and J. Cardy, Entanglement entropy and quantum field theory, *Journal of Statistical Mechanics: Theory and Experiment* **2004**, P06002 (2004).
- [63] J. I. Latorre and A. Riera, A short review on entanglement in quantum spin systems, *Journal of Physics A: Mathematical and Theoretical* **42**, 504002 (2009).
- [64] P. Calabrese and J. Cardy, Entanglement entropy and conformal field theory, *Journal of Physics A: Mathematical and Theoretical* **42**, 504005 (2009).
- [65] K. J. Satzinger, Y.-J. Liu, A. Smith, C. Knapp, M. Newman, C. Jones, Z. Chen, C. Quintana, X. Mi, A. Dunsworth, C. Gidney, I. Aleiner, F. Arute, K. Arya, J. Atalaya, R. Babbush, J. C. Bardin, R. Barends, J. Basso, A. Bengtsson, A. Bilmes, M. Broughton, B. B. Buckley, D. A. Buell, B. Burkett, N. Bushnell, B. Chiaro, R. Collins, W. Courtney, S. Demura, A. R. Derk, D. Eppens, C. Erickson, L. Faoro, E. Farhi, A. G. Fowler, B. Foxen, M. Giustina, A. Greene, J. A. Gross, M. P. Harrigan, S. D. Harrington, J. Hilton, S. Hong, T. Huang, W. J. Huggins, L. B. Ioffe, S. V. Isakov, E. Jeffrey, Z. Jiang, D. Kafri, K. Kechedzhi, T. Khattar, S. Kim, P. V. Klimov, A. N. Korotkov, F. Kostritsa, D. Landhuis, P. Laptev, A. Locharla, E. Lucero, O. Martin, J. R. McClean, M. McEwen, K. C. Miao, M. Mohseni, S. Montazeri, W. Mruczkiewicz, J. Mutus, O. Naaman, M. Neeley, C. Neill, M. Y. Niu, T. E. O'Brien, A. Opremcak, B. Pat'ò, A. Petukhov, N. C. Rubin, D. Sank, V. Shvarts, D. Strain, M. Szalay, B. Villalonga, T. C.

White, Z. Yao, P. Yeh, J. Yoo, A. Zalcman, H. Neven, S. Boixo, A. Megrant, Y. Chen, J. Kelly, V. Smelyanskiy, A. Kitaev, M. Knap, F. Pollmann, and P. Roushan, Realizing topologically ordered states on a quantum pro-

cessor, *Science* **374**, 1237 (2021).
[66] S. Bhattacharjee and A. Dutta, Dynamical quantum phase transitions in extended transverse ising models, *Phys. Rev. B* **97**, 134306 (2018).